Removal of the infrapatellar fat pad and associated synovium benefits female guinea pigs in the Dunkin Hartley model of idiopathic osteoarthritis

Maryam F. Afzali[1]^, Madeline M. Sykes[1], Lindsey H. Burton[2]^, Kayley M. Patton[1], Koryn R. Lee[1], Cassie Seebart[1], Nicole Vigon[3], Ryan Ek[3], Gerardo E. Narez[3], Angela J. Marolf[4]^, Katie J. Sikes[2]^, Tammy L. Haut Donahue[5]^, Kelly S. Santangelo[1]^

[1]Department of Microbiology, Immunology and Pathology, College of Veterinary Medicine and Biomedical Sciences, Colorado State University, Fort Collins, CO, USA; [2]Department of Clinical Sciences, C. Wayne Mcllwraith Translational Medicine Institute, Colorado State University, Fort Collins, CO, USA; [3]Department of Biomedical Engineering, S631 Life Sciences Laboratory, University of Massachusetts Amherst, Amherst, MA, USA; [4]Department of Veterinary Clinical Sciences, College of Veterinary Medicine, The Ohio State University, Columbus, OH, USA; [5]Biomedical Engineering Department, The University of Memphis, Memphis, TN, USA

Contributions: (I) Conception and design: KS Santangelo, MF Afzali, TL Haut Donahue; (II) Administrative support: KS Santangelo, MF Afzali, TL Haut Donahue; (III) Provisions of study materials: KS Santangelo, MF Afzali, TL Haut Donahue; (IV) Collection and assembly of data: MF Afzali, MM Sykes, LH Burton, KM Patton, C Seebart, N Vigon, R Ek, GE Narez, AJ Marolf; (V) Data analysis and interpretation: MF Afzali, MM Sykes, KM Patton, KJ Sikes, TL Haut Donahue, KS Santangelo; (VI) Manuscript writing: All authors; (VII) Final approval of the manuscript: All authors.

Correspondence to: Kelly S. Santangelo, DVM, PhD, DACVP. Department of Microbiology, Immunology and Pathology, College of Veterinary Medicine and Biomedical Sciences, Colorado State University, Pathology 216, 200 West Lake Street, Fort Collins, CO 80523-1619, USA. Email: Kelly.Santangelo@colostate.edu.

Background: Several tissues contribute to the onset and advancement of knee osteoarthritis (OA). One tissue type that is worthy of closer evaluation, particularly in the context of sex, is the infrapatellar fat pad (IFP). We previously demonstrated that removal of the IFP had short-term beneficial effects for a cohort of male Dunkin-Hartley guinea pigs. The present project was designed to elucidate the influence of IFP removal in females of this OA-prone strain. It was hypothesized that resection of the IFP would reduce the development of OA in knees of a rodent model predisposed to the disease.

Methods: Female guinea pigs (n=16) were acquired at an age of 2.5 months. Surgical removal of the IFP and associated synovium complex (IFP/SC) was executed at 3 months of age. One knee had the IFP/SC resected; a comparable sham surgery was performed on the contralateral knee. All animals were subjected to voluntary enclosure monitoring and dynamic weight-bearing, as well as compulsory treadmill-based gait analysis monthly; baseline data was collected prior to surgery. Guinea pigs were euthanized at 7 months. Knees from eight animals were evaluated via histology, mRNA expression, and immunohistochemistry (IHC); knees from the remaining eight animals were allocated to microcomputed tomography (microCT), biomechanical analyses (whole joint testing and indentation relaxation testing), and atomic absorption spectroscopy (AAS).

Results: Fibrous connective tissue (FCT) replaced the IFP/SC. Mobility/gait data indicated that unilateral IFP/SC removal did not affect bilateral hindlimb movement. MicroCT demonstrated that osteophytes were not a significant feature of OA in this sex; however, trabecular thickness (TbTh) in medial femorae decreased in knees containing the FCT. Histopathology scores were predominantly influenced by changes in the lateral tibia, which demonstrated that histologic signs of OA were increased in knees containing the native IFP/SC versus those with the FCT. Similarly, indentation testing demonstrated higher instantaneous and equilibrium moduli in the lateral tibial articular cartilage of control knees with native IFPs. AAS of multiple tissue types

^ ORCID: Maryam F. Afzali, 0000-0002-1053-2612; Lindsey H. Burton, 0000-0002-8791-0239; Angela J. Marolf, 0000-0003-0666-1435; Katie J. Sikes, 0000-0002-3750-4777; Tammy L. Haut Donahue, 0000-0001-7129-9503; Kelly S. Santangelo, 0000-0002-2348-594X.

associated with the knee revealed that zinc was the major trace element influenced by removal of the IFP/SC.

Conclusions: Our data suggest that the IFP/SC is a significant component driving knee OA in female guinea pigs and that resection of this tissue prior to disease has short-term benefits. Specifically, the formation of the FCT in place of the native tissue resulted in decreased cartilage-related OA changes, as demonstrated by reduced Osteoarthritis Research Society International (OARSI) histology scores, as well as changes in transcript, protein, and cartilage indentation analyses. Importantly, this model provides evidence that sex needs to be considered when investigating responses and associated mechanisms seen with this intervention.

Keywords: Osteoarthritis (OA); infrapatellar fat pad (IFP); female Dunkin Hartley guinea pig; biomechanics; trace elements

Submitted Oct 18, 2023. Accepted for publication Apr 10, 2024. Published online Jun 05, 2024.
doi: 10.21037/atm-23-1886
View this article at: https://dx.doi.org/10.21037/atm-23-1886

Introduction

Primary osteoarthritis (OA), particularly knee OA, is the most common form of arthritis and is one of the leading causes of disability worldwide (1,2). The pathogenesis of OA is multifactorial and inter-related, involving structural degeneration and inflammation in multiple tissue types such as cartilage, bone, synovium, adipose depots, menisci, and ligaments (3,4). Of these, there has been growing interest in the infrapatellar (Hoffa's) fat pad (IFP) in knee OA research. The IFP is the most substantial adipose deposit in the knee joint and is most similar in type to white adipose tissue or subcutaneous fat (5,6). However, contribution of the IFP to joint homeostasis is not completely understood. It is postulated to provide lubrication, shock absorption, and/or joint stability to the knee (7-9). Additionally, OA pathology as it relates to the IFP is characterized by a decrease in size and increase in fibrosis and vascularization (10). Fontanella *et al*. (11) have also shown that mechanical properties of the IFP in OA affect the stability and force distribution within the joint, in addition to hindering movement. Lastly, the IFP and synovial membrane has been noted to function as an anato-functional unit (12) and age-dependent tissue remodeling occurs with OA (13).

In addition to the above, there is also potential cross-talk between this depot and other articular tissues in the knee joint. Both adipocytes and immune cells (13,14) in the IFP can initiate cascades of inflammatory mediators, including chemokines, adipokines (i.e., leptin and adiponectin), and cytokines (14,15). Indeed, Klein-Wieringa *et al.* (14) characterized the immune cell fraction of the IFP, revealing a more inflammatory phenotype when compared to subcutaneous adipose tissue (16,17). Others have suggested that the IFP contributes to knee OA by emitting fatty acids and oxylipins (18). Due to the close proximity of the IFP to the synovial membrane, it has also been implied that the IFP could induce OA synovitis. One study (19) compared

Highlight box

Key findings

- The infrapatellar fat pad/synovium complex (IFP/SC) is a significant component driving knee osteoarthritis (OA) in female guinea pigs and that resection of this tissue prior to disease has short-term benefits.

What is known and what is new?

- The IFP has been previously investigated for its involvement in primary OA due to inter-communication between this depot and other components in the knee. Both immune cells and adipocytes are initiators of various inflammatory mediators, including chemokines, adipokines (i.e., leptin and adiponectin), and cytokines that may contribute to disease pathogenesis. Indeed, the IFP may have a more inflammatory phenotype when compared to subcutaneous adipose tissue.
- This manuscript provides results specific to a female cohort of OA-prone Hartley guinea pigs, offering evidence that the IFP/SC has a detrimental influence on disease development in this animal model.

What is the implication, and what should change now?

- The formation of fibrous connective tissue in place of the IFP/SC resulted in decreased cartilage-related OA changes, as demonstrated by reduced histopathology scores, altered transcript/protein expression, and differing mechanical properties. Importantly, these findings were similar but not identical to those elucidated in a male cohort, providing evidence that sex should be considered when investigating responses and associated mechanisms seen with IFP/SC removal.

the response of fibroblast-like synoviocytes (FLS) to conditioned media exposed to either IFP or subcutaneous adipose tissue from patients with advanced knee OA. Their results showed that the extent of inflammatory stimulation was increased with IFP conditioned medium versus that of subcutaneous conditioned medium. Cumulatively, these findings suggest that the IFP has a potential role in patients with severe knee OA.

Briefly, the Dunkin Hartley guinea pig is a recognized model of knee OA, with histopathologic lesions analogous to those found in humans (20). Recently, we published a study in male guinea pigs of this strain which demonstrated that removal of the IFP and its associated synovium complex (IFP/SC) decreased the inflammatory response and transformed biomechanical properties of articular cartilage on the medial tibial plateau (21). This resulted in short-term (4 months) improvement in knee OA. Given these promising data, we then aimed to explore whether this same benefit may be observed in a female cohort of guinea pigs.

Women have a higher risk for OA, with OA-affected women outnumbering OA-affected men at a ratio of approximately 2:1 (22). Previous studies have provided evidence that some etiological pathways proposed to contribute to the disorder might be more predominant in one sex over the other (23-26). For example, metabolic-associated OA is hypothesized to be female-specific (27). Indeed, prevalence of metabolic syndrome differs between sexes, with its clinical representation/manifestation influencing fat distribution and adipocyte function (28). In reference to the IFP, one clinical study suggested that the size of the IFP, as assessed via magnetic resonance imaging, could be associated with symptoms and cartilage damage in older women (29). Specifically, reported maximal IFP areas in women was significantly, and negatively, associated with changes in knee pain. In contrast, findings suggested that maximal IFP area in females was beneficially associated with medial and lateral tibial cartilage volume and reduced risk of medial cartilage defects (femoral and tibial). These potentially dichotomous indications highlight the unknown influence of the IFP in female patients and the need to further dissect biological mechanisms and/or relationships among joint tissues.

Thus, the current work attempted to elucidate the influence that unilateral IFP/SC removal would have on the onset of knee OA in female Dunkin Hartley guinea pigs. There were two immediate aims relevant to this work: (I) to determine whether mobility changes (open-field enclosure monitoring, treadmill based gait and voluntary weight bearing analyses), an indication of modification in clinical signs, were present; and (II) to evaluate potential disease modification {assessed via structural [histopathology, microcomputed tomography (microCT), transcript and protein assessment] and biomechanical [whole joint, indentation relaxation testing and atomic absorption spectroscopy (AAS)] outcomes} after surgical resection of the IFP/SC. We hypothesized that the IFP/SC is a local supply of negative mediators (21) and that, through surgical resection, we might achieve short-term improvements for OA pathogenesis. We present this article in accordance with the ARRIVE reporting checklist (available at https://atm.amegroups.com/article/view/10.21037/atm-23-1886/rc).

Methods

Animals

Experiments were performed under a project license (#15-5854A; October 30, 2021) granted by Colorado State University's Institutional Animal Care and Use Committee, in compliance with the NIH Guide for the Care and Use of Laboratory Animals.

Sixteen 8-week-old, female guinea pigs were supplied by a commercial vendor (Charles River Laboratories, Wilmington, MA, USA). Animals were housed 4 weeks prior to surgery at the university's animal facilities and checked daily. All guinea pigs were singly housed under a 12/12-h light/dark cycle at 20–26 ℃ with 30–70% humidity. Water, pelleted food, and hay cubes were offered *ad libitum* and weights were recorded weekly.

Two cohorts were utilized to achieve the outcomes of this study. Separate groups of animals were obtained for histological and molecular-based properties of knees (first cohort; n=8) versus biomechanical assessments (second cohort; n=8). Both cohorts were evaluated for mobility outcomes (treadmill-based gait, voluntary dynamic weight bearing, and overhead monitoring). A group size of n=8 was prospectively determined from the published male cohort study using histopathology as the main outcome (21). An untreated control group of eight female Hartley guinea pigs at a matching age and from the identical vendor—from a parallel but separate project—was used for body weight (BW) and overhead enclosure monitoring comparisons.

Unilateral surgical removal of the IFP/SC

Dunkin Hartley guinea pigs begin to present OA pathogenesis

at 16 weeks of age. Removal of the IFP/SC from right knees was executed on 12-week-old guinea pigs, which is prior to the development of OA in this model. Animals were induced to an anesthetic plane using 3–4% inhaled isoflurane in oxygen, followed by maintenance with 2–3% isoflurane. Slow release buprenorphine at a dose of 0.8 mg/kg was provided as a pre-medication. The right knee was opened via parapatellar arthrotomy and the patella was displaced cranially with the knee in extension to allow access to the IFP/SC. This tissue was then exposed medially for dissection and removal. The skin incision was closed with absorbable suture after repositioning of the patella. A matching control procedure on left knees—with gentle handling of the IFP/SC via forceps but without removal—was performed and served as an internal control for each animal.

Symptom modification

Guinea pigs were familiarized to the three systems over 2 weeks. Data collection was performed by a single handler during a consistent time (8:00 AM to 12:00 PM); animals were randomly selected for analysis. Baseline data was collected the day prior to IFP/SC resection. Longitudinal data were gathered monthly following surgery, with the last time point collected the day before termination (16 weeks post-surgery). Each outcome was performed on a separate day of the week with at least one day between each handling. Data for each mobility assessment parameter is absent for all guinea pigs at 12 weeks post-operatively due to coronavirus disease 2019 (COVID-19) pandemic restrictions.

Open-field enclosure monitoring

Voluntary physical mobility was performed for 10 minutes using an automated behavior monitoring system (ANY-Maze^{TM}, Wood Dale, IL, USA) (30,31). The enclosure was a circular, blue plastic bin measuring 114 cm in diameter and 15 cm in height; the animal's individual red hut shelter was placed in the center for each recording.

Treadmill-based gait analyses

The DigiGait^{TM} treadmill system (Mouse Specifics, Inc., Framingham, MA, USA) was used to assess obligatory gait patterns (21). Animals were recorded in the dark at a treadmill speed of 45 cm/s to collect one run that contained a minimum of five consecutive steps without acceleration or deceleration. Mean values were analyzed for each parameter of interest.

Voluntary weight-bearing analyses

Voluntary weight-bearing was collected using a Rodent Walkway System (Tekscan, South Boston, MA, USA) (21). Guinea pigs were recorded naturally traversing the Tekscan walkway for 3 times/day; parameters focused on maximum force, force time impulse, and maximum force symmetry values (front/hind, left/right, left front/right front, left hind/right hind). As for compulsory gait analysis, mean values were used in statistical comparisons for each parameter of interest.

Tissue collection

Humane euthanasia occurred when animals were 7-month-old. BWs were recorded; left and right femurs were measured in millimeters from the proximal aspect of the greater trochanter to the apex of the patella using calipers. For the first set of animals (n=8), both hindlimbs were fixed in 10% neutral buffered formalin for 48 hours; specimens were placed phosphate buffer saline (PBS) for microCT. After imaging, limbs were decalcified in 12.5% solution of ethylenediaminetetraacetic acid (EDTA) at pH 7 for subsequent histology. For animals designated to the second cohort (n=8), hindlimbs were frozen at –20 ℃ following femur measurements; quantitative microCT was performed after complete thaw, followed immediately by biomechanical outcomes.

MicroCT

Left (native IFP/SC) and right (IFP/SC removal) knee joints from the first cohort, which were dedicated to histology and molecular analysis (n=8 animals), were scanned using the Inveon microPET/CT system (Siemens Medical Solutions, Malvern, PA, USA) for 1356 ms at 10 kV with a voxel size of 18 mm. A blinded board-certified veterinary radiologist (A.J.M.) scored evidence of OA (32).

Left and right knee joints allocated to biomechanical outcomes (n=8 animals) were scanned using the Bruker Skycan 1276 (Bruker, Billerica, MA, USA) for 473 ms at 100 kV with a voxel size of 20 mm. Osteophytes were manually outlined by the same operator (G.E.N.) (21). Four regions of interest (ROI) consistent with areas of mechanical testing were evaluated (33-36). Trabecular and cortical bone volumes of interests (VOIs) were identified, as previously described (21).

Histopathologic scoring of OA

Decalcified knees were paraffin embedded and sagittally sectioned at 5-microns through three regions: (I) mid-sagittal slices were made to evaluate the IFP/SC with hematoxylin and eosin (H&E); and sagittal slices through both the (II) medial and (III) lateral compartments were stained with toluidine blue to assess OA using Osteoarthritis Research Society International (OARSI) recommended criteria (20). Two blinded, independent evaluators (M.F.A. and K.S.S.) completed histological scoring; any minor differences in scoring were resolved prior to statistical analysis. A total knee OA score for each hindlimb was obtained from adding scores for the medial/lateral tibiae and medial/lateral femorae.

Transcript expression

Total RNA was collected (Roche, Basel, Switzerland) from either the IFP/SC or replacement tissue that remained in blocks after collecting sufficient sections for joint histology and immunohistochemistry (IHC); 800 ng of total RNA was hybridized at 65 ℃ with the custom code-set followed by processing on the NanoString nCounter FLEX Analysis system (NanoString Technologies, Seattle, WA, USA). A custom set of guinea pig-specific probes were designed and manufactured by NanoString Technologies for the following genes: adiponectin (*ADIPOQ*), leptin (*LEP*), fatty acid synthetase (*FASN*), cell death-inducting DFFA-like effector c (*CIDEC*; also known in rodents as *Fsp27* or fat-specific protein 27), mitogen-activated protein kinase (*MAPK*), kelch-like ECH-associated protein-1 (*KEAP1*), Rho-family-alpha serine/threonine-protein kinase (*AKT*), catalase (*CAT*), glutathione peroxidase (*GPx*), complement component 3 (C3), and matrix metallopeptidase-2 (*MMP-2*), tissue inhibitor of metalloproteinases 2 (*TIMP-2*), and nitric oxide synthase (*NOS3*). The complete custom gene panel is provided in Table S1. Absolute transcript counts were normalized to three housekeeping genes (b-actin, succinate dehydrogenase, and glyceraldehyde-3-phosphate dehydrogenase) and positive controls. Data analysis was conducted using nSolver software (NanoString Technologies).

IHC analysis

Protein expression via IHC was conducted on mid-sagittal sections or sagittal slices through the lateral compartment. Polyclonal rabbit antibodies to *TIMP-2* (2.5 mg/mL, Abcam ab180630) or a disintegrin and metalloproteinase with thrombospondin motifs-4 (*ADAMTS-4*; 2.5 mg/mL, Abcam ab185722). Briefly, tissue underwent antigen retrieval (5 hours at 55 ℃), blocking with 2.5% normal goat serum, overnight humified incubation at 4 ℃ with primary antibody (37), and exposure to biotinylated goat anti-rabbit secondary antibody for 30 minutes. Tissues were counterstained with hematoxylin. Integrated optical density was determined on four 1-mm-square regions using ImagePro-Plus 7 Software (Media Cybernetics, Rockville, MD, USA); data was averaged prior to statistical analysis. Background staining was negligible with negative controls (rabbit immunoglobulin at 2.5 µg/mL or secondary antibody, alone).

Biomechanical analyses

Whole joint testing

This testing evaluated the overall behavior of the joint, as well as the failure characteristics of the IFP/SC or FCT. Briefly, femorae and tibiae were potted in epoxy resin. A servo-hydraulic testing system (MTS, Eden Prairie, MN, USA) with an 8.9 N load cell was utilized for: (I) an anterior/cranial drawer assessment for total displacement of the tibia relative to the femur; and (II) a pull-to-failure test of the patellar tendon and associated underlying structures (IFP/SC or FCT). Pull-to-failure was assessed by dragging the tibia to 4 N of drawer at 0.5 mm/s.

Indentation relaxation testing

Indentation relaxation tests were performed on a servo-hydraulic testing system (MTS Corp.) and 9 N load cell (Futek, Irvine, CA, USA). Indentation relaxation tests were performed on cartilage and menisci in a phosphate-buffered saline bath to determine instantaneous and equilibrium moduli, as per previous work (21).

AAS

Trace elements were measured to provide potential explanations for differences detected by whole joint or indentation relaxation testing. Calcium (Ca), iron (Fe), magnesium (Mg), phosphorus (P), and zinc (Zn) quantifications, which are major trace elements that have been associated with alterations in tissue properties (21), were performed on freeze-thawed tissue samples dedicated to biomechanical analyses (n=8 animals), including: (I) the IFP/SC or replacement tissue; (II) articular cartilage

from the tibia and femur (separated into medial and lateral compartments); (III) patellar tendon; (IV) patella; and (V) separated distal medial and lateral femoral condyles, representing combined cortical and subchondral trabecular bone. Dried samples were handled as previously described (21,38). Trace element levels were calculated as parts per million (ppm) dry weight (dw) (38).

Statistical analyses

Exclusion criteria were determined prior to analysis. Justification for exclusions and total number analyzed for data sets are provided in Table S2.

Statistical analyses were performed was performed using GraphPad Prism 10.1.1 for Mac OS X, GraphPad Software, (Boston, MA, USA, www.graphpad.com) with significance set at P<0.05. Normality and variance were assessed with the Shapiro-Wilk test. Normally distributed data with similar variance were compared using paired *t*-test; non-normally distributed data underwent the Wilcoxon matched-pairs signed rank test. Two-way analysis of variance (ANOVA or Mixed Model) with Tukey *post hoc* test analyses were performed on longitudinal mobility data.

Results

Study animal description

BWs were recorded weekly for the duration of the study (Figure S1A); no issues of clinical concerns were noted. BW at harvest was not significantly different from 7-month-old female untreated controls in a separate but simultaneous study (Figure S1B). Mean BW was 969 g [95% confidence interval (CI): 930–1,009] in the IFP/SC removal group and 946 g (95% CI: 899–992) in the control group.

Left (native IFP) and right (IFP/SC removal) femurs lengths from all guinea pigs were measured. Femur lengths between the left (mean =40.73 mm; 95% CI: 37.94–43.59) and right (mean =40.37; 95% CI: 37.91–43.60) hindlimbs were not significantly different (P=0.89) (Figure S1C).

Movement/mobility assessment

Open-field enclosure monitoring

To assess whether removal of the IFP impacted overall animal voluntary movement/mobility, open-field enclosure monitoring was utilized (*Figure 1A*). At time of termination (7 months of age), there was a significant increase in average speed (P<0.01), total distance traveled (P<0.01), and total time mobile (P<0.01) in animals receiving IFP/SC removal when compared to control guinea pigs with no surgical intervention (*Figure 1B-1D*). Correspondingly, guinea pigs with surgical interventions also observed a significant decrease in time spent in their red hut (P<0.001; *Figure 1E*).

Treadmill-based gait analyses

A description of gait parameters can be found in a companion manuscript focused on male animals (21). Significant differences were noted over time for stride length (cm) (P<0.001), stance (P<0.001), and propel time (P<0.01) due to an expected increase in size with aging. Notably, no differences were seen for remaining parameters between the IFP/SC removal and contralateral sham control hindlimbs (*Figure 1F-1K*).

Voluntary weight-bearing analyses

Gait metrics analyzed via voluntary dynamic weight-bearing were consistent with treadmill-based gait results, including stride length, stride time, stance time and swing time. Additional parameters identified by this technique that were associated with aging over time included significant differences for maximum force and stride velocity (P<0.001). Comprehensive voluntary dynamic weight-bearing parameters are supplied in Table S3.

As for treadmill-based gait, no significant differences were found for fore/hind symmetry, maximum force (%BW), or stride velocity (cm/s) between IFP/SC removal and contralateral sham control hindlimbs (*Figure 1L-1N*).

Description of IFP/SC versus replacement tissue

Morphologic description

Knees containing the native tissue maintained the cellular properties expected of IFP/SC, including mature adipocytes (A), a stromal vascular fraction (SVF), and occasional white blood cells [large and small mononuclear (LM and SM) cells, consistent with macrophages and lymphocytes, respectively] (*Figure 2A,2B*). Conversely, IFP/SC removal knees developed a thick band of dense fibrous connective tissue (FCT) in the location typically inhabited by the IFP/SC (*Figure 2C,2D*). Of note, intact synovium was present in all specimens.

Transcript analyses

Components/regulators of adipose tissue

The FCT had a lower expression of transcripts for *ADIPOQ*

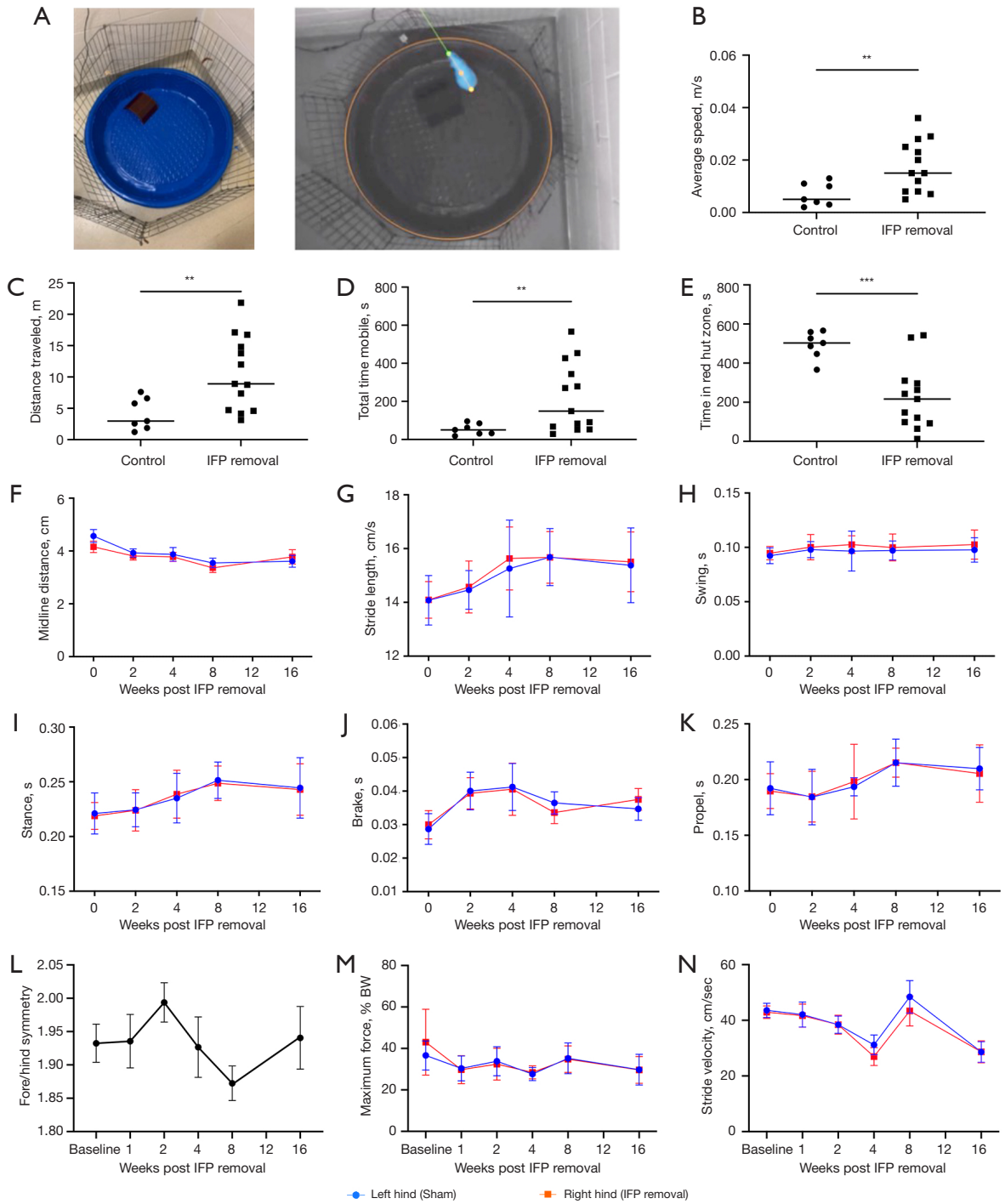

Figure 1 Symptom modification. Image of open-field enclosure system; video still image (A) showing a guinea pig with tracking system (viewed from above). Final timepoints comparison of IFP/SC removal (n=13) to 7 months of age guinea pigs (n=7) average speed (B), total distance traveled (C), total time mobile (D), and time in red hut zone (E). Longitudinal data of IFP/SC (blue) and FCT (n=12) (red) for midline distance (F), stride length (G), swing (H), stance (I), brake (J) and propel time (K). Voluntary weight-bearing (n=16) between fore/hind symmetry (L), maximum force [% BW, (M)], and stride velocity (N). P values represent significance of two-way ANOVA or Mixed Model with Tukey *post hoc* test analyses. **, P<0.01; ***, P<0.001. IFP, infrapatellar fat pad; IFP/SC, infrapatellar fat pad/synovium complex; FCT, fibrous connective tissue; BW, body weight; ANOVA, analysis of variance; s, seconds; m, meters; cm, centimeters.

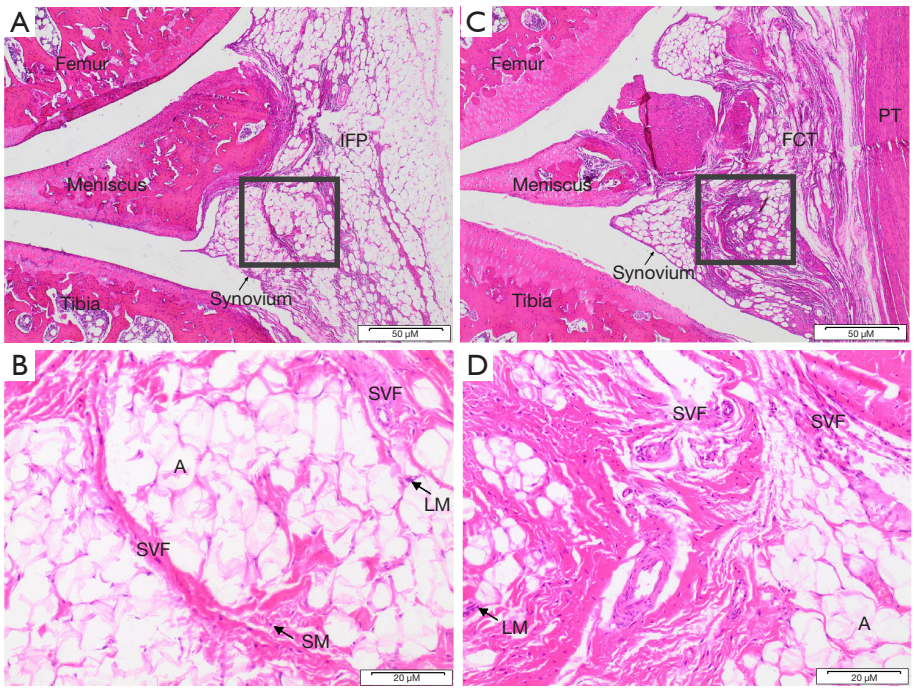

Figure 2 Characterization of IFP/SC and replacement tissue. 2× objective (H&E, 50 µM) representative images of a knee joint from a control (A,B) and IFP/SC removal (C,D) guinea pig (A,C); squares indicate magnified views (B,D) with the 20× objective (20 µM). Dense FCT (D) replaced the IFP/SC (B). PT, SVF; mature adipocytes (A), SM, LM cells. IFP, infrapatellar fat pad; FCT, fibrous connective tissue; PT, patellar tendon; SVF, stromal vascular fraction; SM, small mononuclear; LM, large mononuclear; A, adipocytes; IFP/SC, infrapatellar fat pad/synovium complex; H&E, hematoxylin & eosin stain.

(P=0.02), *LEP* (P=0.01), *FASN* (P=0.05) and *CIDEC* (P=0.01) compared to the native IFP/SC (*Figure 3A-3D*).

Inflammatory mediators and antioxidant enzymes

The FCT also had decreased expression of mRNA for *MAPK* (P=0.02), *C3* (P=0.03), *KEAP1* (P=0.03), *GPx* (P=0.03), *NOS3* (P=0.02); and *CAT* (P<0.001) (*Figure 3E-3J*).

Degradative mediators

Relative to the IFP/SC, the FCT had increased mRNA expression for *MMP-2* (P=0.03) and *TIMP-2* (P=0.03) (*Figure 3K,3L*).

IHC for remodeling

MMP Inhibitor

To support the mRNA data, *TIMP-2* was evaluated at the protein level in the native IFP/SC versus the FCT (*Figure 3M-3O*). *TIMP-2* immunostaining was significantly higher in the FCT (P=0.02).

Degradative mediator

Primary aggrecanases ADAMTS (ADAM with thrombospondin motifs)-4 and -5 are key degradative metalloproteinases that are inhibited by TIMPs (39) and are relevant in OA (40). Protein expression of the aggrecanase ADAMTS-4 was thus evaluated using IHC. Relative to limbs containing the native IFP/SC, ADAMTS-4 was significantly decreased in limbs with the FCT (P<0.01; *Figure 3P-3R*).

Biomechanical analyses and AAS for trace elements

Whole joint mechanical testing was performed to determine whether the presence of the IFP/SC versus FCT altered cranial/anterior drawer assessment. No significant changes were detected between the IFP/SC and FCT (Table S4), which was expected given that this is primary assessment of the integrity of the cranial/anterior cruciate ligament. There were also no statistical differences in trace element concentrations between the IFP/SC and FCT (Table S5).

Pull to failure testing of the patellar tendon and associated caudal/posterior tissue was then performed to determine if the IFP/SC versus FCT altered outcomes. Elastic modulus from pull to failure testing was significantly decreased in the FCT (P<0.01) when compared to the IFP/SC (*Figure 4A*; Table S4). To determine whether tissue

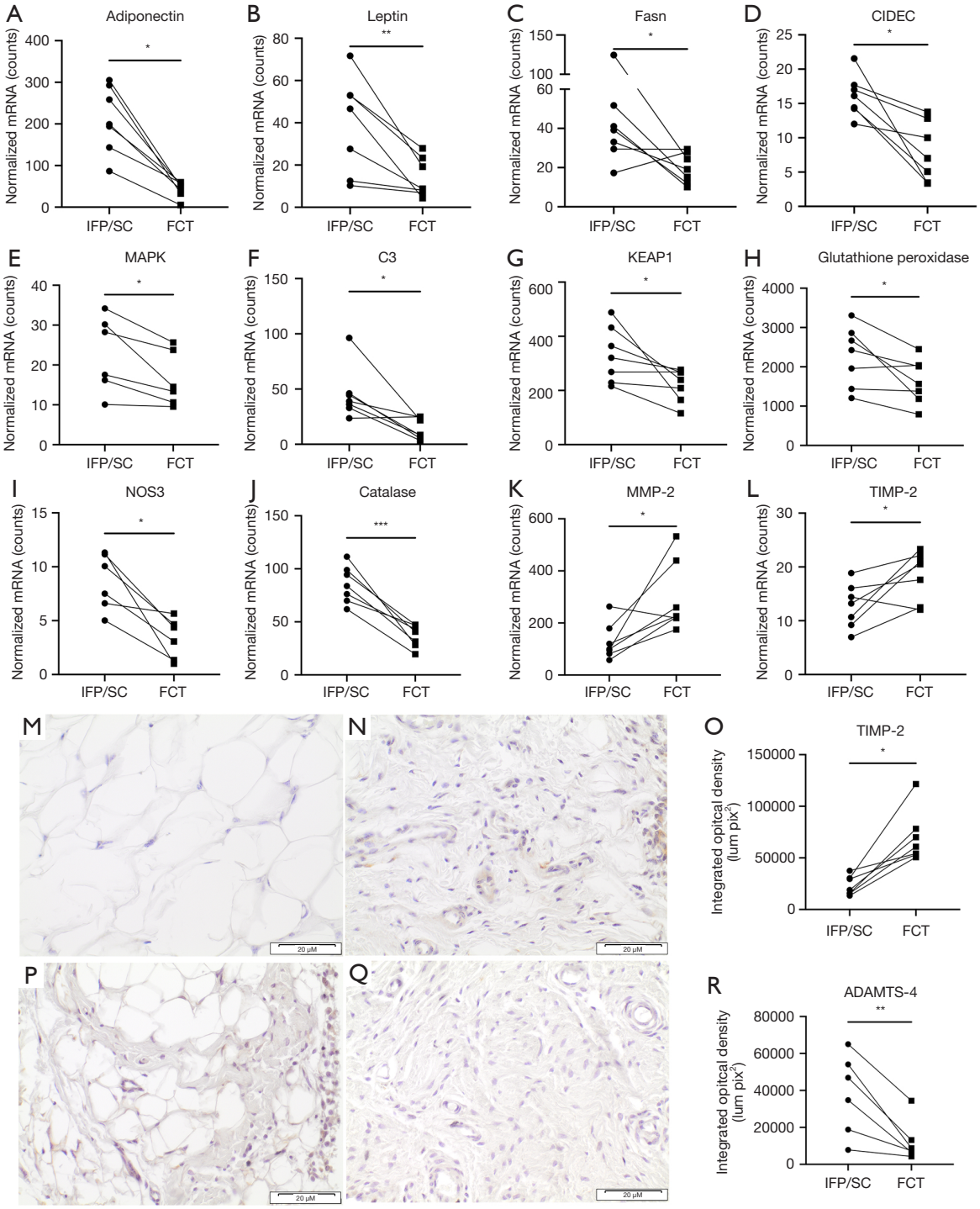

Figure 3 mRNA and protein expression. Normalized transcript counts (n=7) for adiponectin (A), leptin (B), FASN (C), CIDEC (D), MAPK (E), C3 (F), KEAP1 (G), GPx (H), NOS3 (I), CAT (J), MMP-2 (K), and TIMP-2 (L) in IFP/SC and FCT of knee joints. DAB staining immunohistochemistry for TIMP-2 signal in IFP/SC (M, left hindlimb) and FCT (N, right hindlimb). TIMP-2 is a potent inhibitor of most MMPs; notably, expression in the FCT was increased [40× objective (20 µM)]. (O) Quantitation of TIMP-2-stained tissue subtracted from IgG control tissue. DAB staining immunohistochemistry for ADAMTS-4 is a major proteinase responsible for degradation of proteoglycans in articular cartilage in OA; protein is higher in IFP/SC (P, left hindlimb) versus FCT (Q, right hindlimb) [40×

objective (20 μM)]. (R) Quantitation of ADAMTS-4 stained tissue normalized to IgG control sections. As all data were non-parametric, comparisons were statistically determined via Wilcoxon matched pairs signed rank test. *, P<0.05; **, P<0.01; ***, P<0.001. IFP/SC, infrapatellar fat pad/synovium complex; FCT, fibrous connective tissue; FASN, fatty acid synthase; CIDEC, cell death-inducting DFFA-like effector c; MAPK, mitogen activated protein kinase; C3, complement component 3; KEAP1, kelch-like ECH-associated protein-1; GPx, glutathione peroxidase; NOS3, nitric oxidase synthase 3; CAT, catalase; MMP-2, matrix metallopeptidase-2; TIMP-2, tissue inhibitor of metalloproteinase-2; DAB, 3,3'-diaminobenzidine; IgG, immunoglobulin G; ADAMTS-4, a disintegrin and metalloproteinase with thrombospondin motifs-4; OA, osteoarthritis.

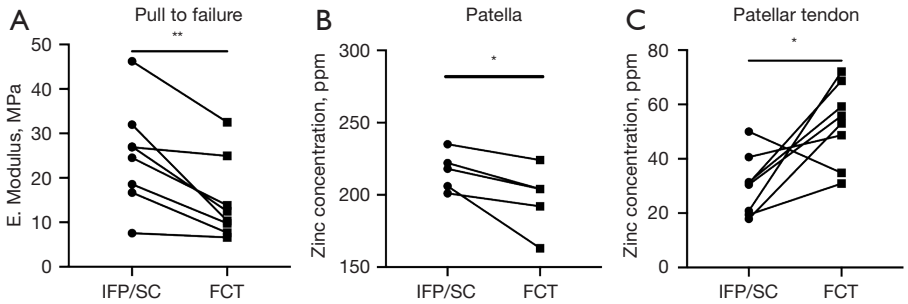

Figure 4 Biomechanical analyses and trace element concentration of tissues. Ultimate tensile strength was tested (n=7). Elastic modulus (A) decreased in the FCT when compared to the IFP/SC hindlimb. Trace element analysis (n=8) of the patella (B) revealed a decrease of Zn concentration in the FCT patella when compared to the IFP/SC. However, patellar tendon (C) from the FCT had higher concentration of Zn compared to the IFP/SC. Data with similar variance and normal distribution were compared using parametric *t*-tests. Wilcoxon matched pairs signed rank test was used to compare data with non-Gaussian distribution. *, P<0.05; **, P<0.01. MPa, megapascal; IFP/SC, infrapatellar fat pad/synovium complex; FCT, fibrous connective tissue; Zn, zinc.

mineralization may have contributed to these differences, trace elements were measured in both patellae and patellar tendons. For the former, patellae in FCT-containing knees had significantly lower concentrations of Zn (*Figure 4B*; P=0.05) compared to those from knees with native IFP/SC. In contrast, patellar tendons from FCT-containing knees had higher concentrations of Zn (*Figure 4C*; P=0.01) when compared to IFP/SC-containing patellar tendons. Additional but nonsignificant trace element concentrations for the patellae and patellar tendons can be found in Tables S6,S7.

Characterization of cartilage and bone pathology

OARSI histology score

Representative images of the lateral tibia plateau of knees from a single guinea pig are seen in *Figure 5A,5B*. The control knee containing the native IFP/SC showed irregular/undulated cartilage with mild fibrillation; decreased proteoglycan content in superficial, middle, and deep zones; and increased hypocellularity (*Figure 5A*). The treated knee containing FCT in lieu of the IFP/SC demonstrated a mild surface irregularity; very mild proteoglycan loss; and slight hypocellularity (*Figure 5B*). Correspondingly, OA scores were significantly different, with the IFP/SC group higher than that of the FCT (*Figure 5C*; P=0.04). When medial (*Figure 5D*) and lateral compartments were considered independently, the lateral compartment was the driver (*Figure 5E*; P=0.01) in the total OARSI score, with the lateral tibia being significantly different (*Figure 5F*; P=0.01) when compared to the lateral femur (*Figure 5G*). Overall, the improved histological scores for the knees with the FCT confirmed a maintenance of cartilage structure, proteoglycan content, and chondrocyte cellularity (*Figure 5H-5K*).

IHC for degradative mediators in lateral tibial plateau cartilage

Similar to the IFP/SC and FCT, immunostaining for TIMP-2 (*Figure 6A-6C*; P=0.02) in the lateral tibial plateau was statistically increased in FCT containing knees. ADAMTS-4 was significantly decreased (*Figure 6D-6F*; P=0.02).

MicroCT

Subjective whole joint OA scores

Clinical OA scores in the guinea pigs dedicated to histology

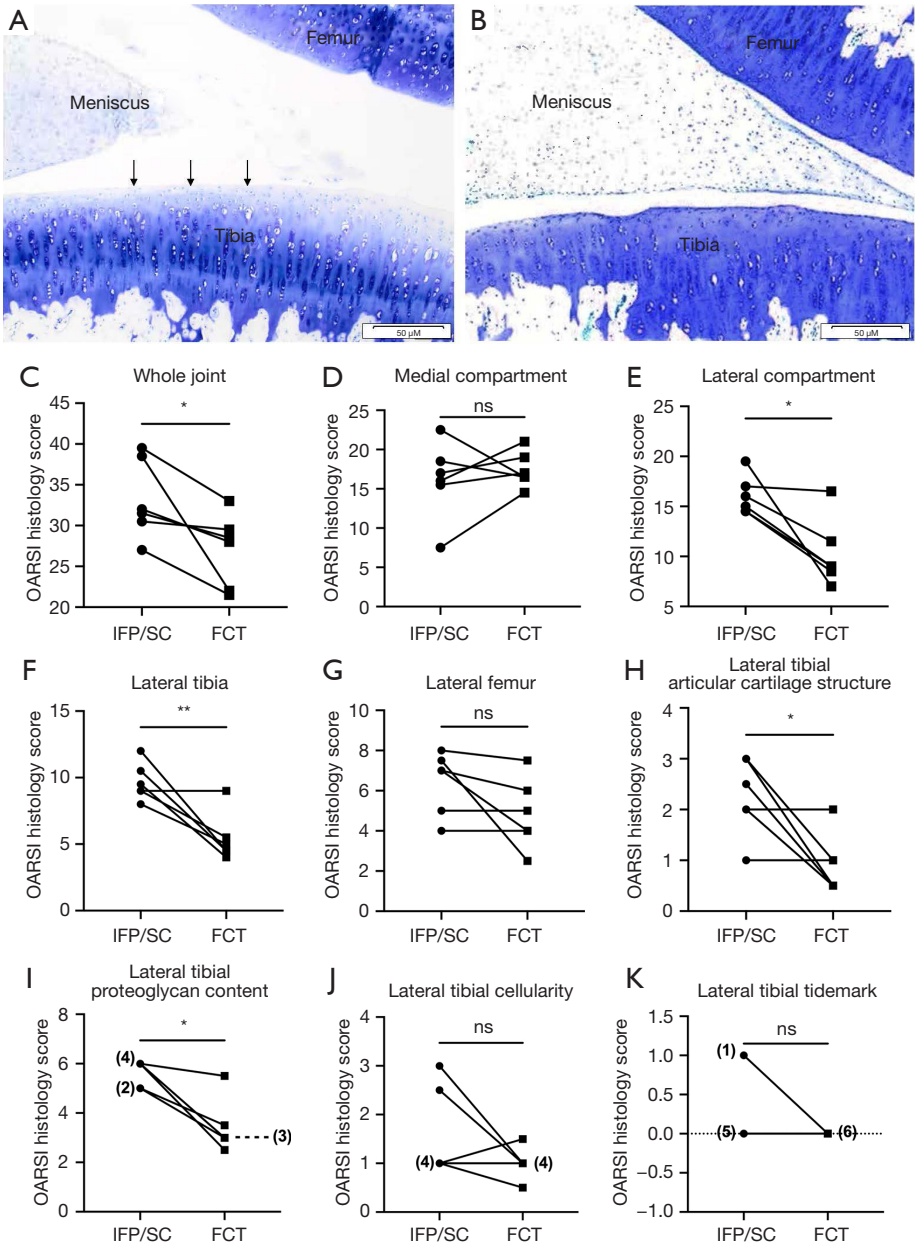

Figure 5 OARSI score. Representative photomicrographs [2× objective (50 µM)] sections of the lateral compartment. (A) Black arrows denote mild fibrillation and proteoglycan loss in the superficial zone of tibial cartilage from the knee containing the IFP/SC. (B) The opposite knee had a smooth cartilage surface with only mild proteoglycan loss. (C) OARSI whole joint OA score (n=6) confirmed a significant statistical difference. Contributing compartments included: the medial compartment (D), which was not significantly different; and the lateral compartment (E), which was significantly different. While the lateral tibia (F) did contribute to score differences, the lateral femur (G) did not contribute to score differences score from FCT-containing knees, which summed articular cartilage structure (H), and proteoglycan content (I) had significantly decreased OA. Cellularity (J) and tidemark (K) did not contribute to the lateral tibial OARSI Score. Data with similar variance and normal distribution were compared using parametric *t*-tests. Wilcoxon matched pairs signed rank test was used to compare data with non-Gaussian distribution. (I-K) The numbers 1–6 indicate number of individual animals at each data point. *, P<0.05; **, P<0.01; ns, no significance. OARSI, Osteoarthritis Research Society International; IFP/SC, infrapatellar fat pad/synovium complex; FCT fibrous connective tissue; OA, osteoarthritis.

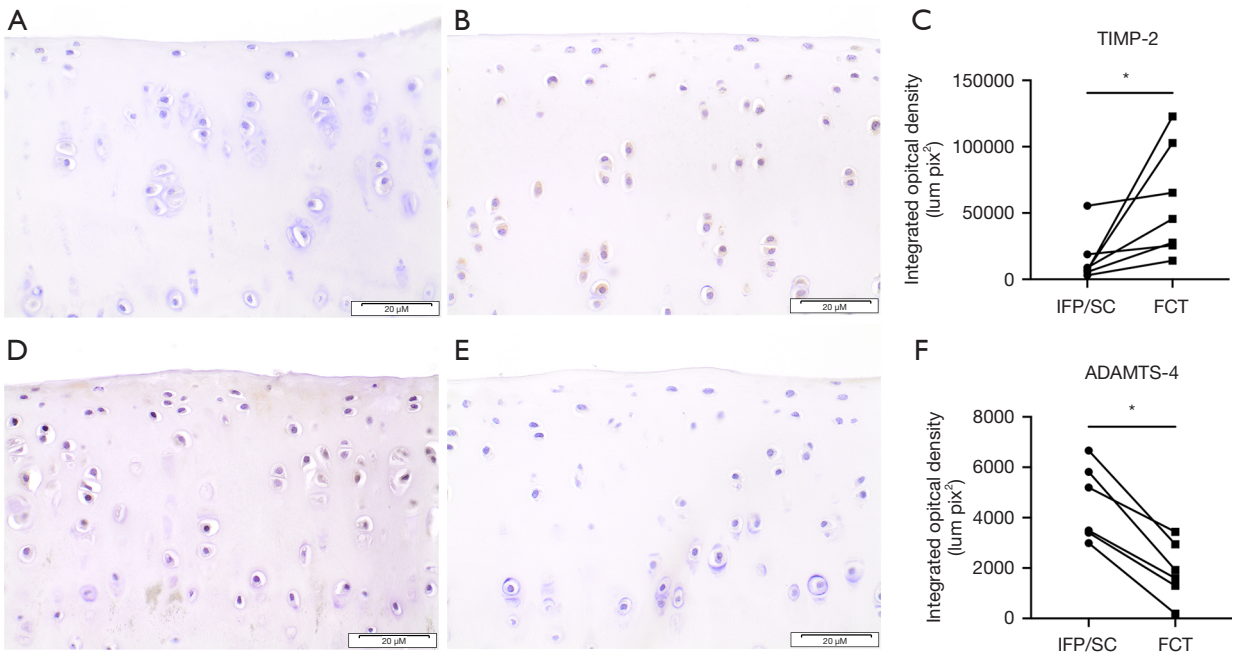

Figure 6 TIMP-2 and ADAMTS-4 IHC of LTP articular cartilage. Representative images of LTP articular cartilage containing DAB immunostaining for TIMP-2 from IFP/SC (A) and FCT (B) containing knees of the same animal [40× objective (20 µM)]. (C) Quantitation of TIMP-2-stained tissue subtracted from IgG control tissue. DAB staining immunohistochemistry for ADAMTS-4 is a major proteinase responsible for degradation of proteoglycans in articular cartilage in OA; protein is higher in IFP/SC (D, left hindlimb) versus FCT (E, right hindlimb) [40× objective (20 µM)]. (F) Quantitation of ADAMTS-4 stained tissue normalized to IgG control sections. Data with similar variance and normal distribution were compared using parametric *t*-tests. *, P<0.05. TIMP-2, tissue inhibitor of metalloproteinase-2; ADAMTS-4, a disintegrin and metalloproteinase with thrombospondin motifs-4; IFP/SC, infrapatellar fat pad/synovium complex; FCT, fibrous connective tissue; IHC, immunohistochemistry; LTP, lateral tibia plateau; DAB, 3,3'-diaminobenzidine; IgG, immunoglobulin G; OA, osteoarthritis.

and molecular analysis (n=8) did not reveal significant bony changes in their tibiae, femurs, or patellae (Table S8). Additionally, differences in osteophyte volumes were not observed (Table S9).

Quantitative microCT

Animals in the biomechanical outcome group (n=8 animals) were analyzed for quantitative microCT. Significant differences were found for trabecular thickness (TbTh) of the medial femur (*Figure 7A*; P=0.01). Additional but nonsignificant parameters measured for quantitative microCT can be found in Table S10. Separate distal medial and lateral femoral condyles, representing both cortical and subchondral trabecular bone, were tested for trace elements to pursue a possible reason for this increase in TbTh for IFP/SC knees (Table S11). Interestingly, trabecular bone from the lateral, but not medial, femoral condyles of IFP/SC-containing knees had significantly decreased Zn (*Figure 7B*; P=0.02); no other differences were noted in cortical and subchondral trabecular bone from the lateral or medial condyles (Table S11).

Biomechanical analyses and AAS for trace elements

Comparative stress-relaxation indentation test for cartilage demonstrated that the instantaneous modulus of the lateral tibial articular cartilage was significantly decreased in the FCT knees (*Figure 8A*; P=0.02). Similarly, there was also a statistically lower equilibrium modulus in the lateral tibia articular cartilage (*Figure 8B*; P=0.03). Additional but nonsignificant meniscus and cartilage indentation analyses can be found in Table S12. Based on these findings, coupled with the OARSI histologic scoring results, lateral tibia articular cartilage was collected for AAS to determine if tissue mineralization in IFP/SC containing knees may be responsible for these findings. Zn was lower in lateral tibia cartilage from FCT-containing knees compared to those with the native IFP/SC (*Figure 8C*; P=0.04). Remaining concentrations (mean values and 95% CIs) for all trace elements tested in the medial and lateral cartilage are

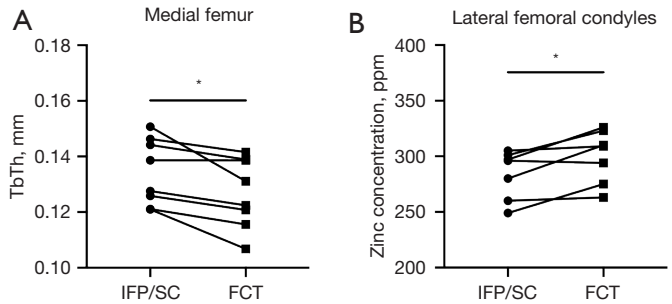

Figure 7 Biomechanical analyses and trace element concentration of IFP/SC *vs*. FCT. Quantitative microCT (n=8) showed decreased trabecular thickness (mm) of the medial femur in the FCT (A) relative to the IFP/SC. Lateral femoral condyles analyzed for trace elements (n=8) revealed a higher abundance of Zn in the trabecular bone of the FCT (B) when compared to the IFP. Data with similar variance and normal distribution were compared using parametric *t*-tests. Wilcoxon matched pairs signed rank test was used to compare data with non-Gaussian distribution. *, P<0.05. IFP/SC, infrapatellar fat pad/synovium complex; FCT, fibrous connective tissue; TbTh, trabecular thickness; ppm, parts per million; microCT, microcomputed tomography; Zn, zinc; mm, millimeters.

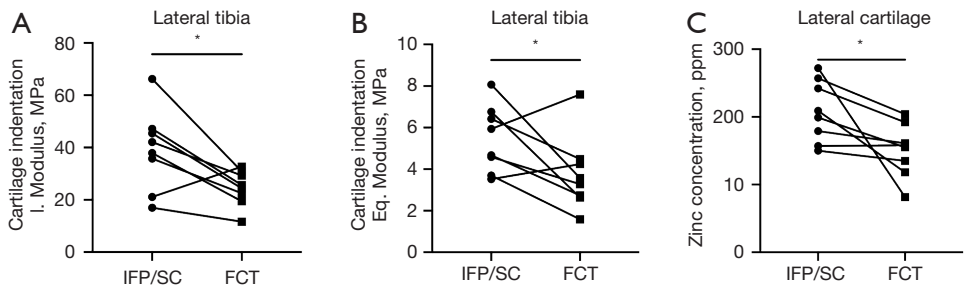

Figure 8 Cartilage indentation and trace element concentration of lateral cartilage. Cartilage indentation (n=7) including: instantaneous modulus (A) and equilibrium elastic modulus (B) of the lateral tibial cartilage were lower in FCT containing knees when compared to the IFP/SC. Lateral cartilage from FCT knees contained lower concentrations of Zn (C) compared to cartilage collected from IFP/SC knees. Data with similar variance and normal distribution were compared using parametric *t*-tests. Wilcoxon matched pairs signed rank test was used to compare data with non-Gaussian distribution. *, P<0.05. MPa, megapascal; IFP/SC, infrapatellar fat pad/synovium complex; FCT, fibrous connective tissue; ppm, parts per million; Zn, zinc.

presented in Tables S13,S14. The medial compartment did not have significant differences in indentation testing or trace element concentrations.

Discussion

The overall goals of this greater study were: (I) to determine whether removal of the IFP/SC in a female cohort of Dunkin Hartley guinea pigs influenced the development of knee OA; and (II) to compare these findings with the results from a corresponding group of males (21). Notably, data from females established that resection of the IFP/SC prior to the onset of OA decreased the development of OA-associated cartilage lesions, which was similar to the published male cohort. However, there were notable differences between the sexes in regards to cartilage and boney changes, gene and protein expression, biomechanical analyses, and trace elements that are worthy of highlighting (*Table 1*).

Movement/mobility assessment

Gait assessment, voluntary movement, and weight bearing assessment in preclinical rodent models of OA has increased in recent years; the field acknowledges the importance/relevance of consideration of gait analyses in existing OA models for the indirect evaluation of symptom modification (41-44). Modification of clinical signs in the current work

Table 1 Sex differences between male and female Dunkin Hartley guinea pigs with surgical removal of the IFP/SC at 4 months of age (prior to OA onset) and aged to 7 months of age (moderate OA). Assessment/outcomes are listed as differences observed in the FCT (IFP removal) hind limb when compared to sham IFP/SC hind limbs

Comparison	Method/assessment	Male cohort (21)	Female cohort
Similar	Treadmill (compulsory mobility)	No unilateral differences between hind limbs	
	Tekscan (voluntary weight bearing)	No unilateral differences between hind limbs	
	Histological changes	IFP/SC was replaced with dense FCT	
Differences	NanoString gene expression IFP/SC *vs.* FCT	Decrease in components of adipose tissue and inflammatory mediators. Increased mRNA expression of degradative mediator MMP-2	Decrease components of adipose tissue, inflammatory mediators and antioxidant enzymes. Increased expression of degradative mediators, TIMP-2 and MMP-2
	Immunohistochemistry, IFP/SC *vs.* FCT	Decrease protein expression of inflammatory mediators, for NF-κB p65 and MCP-1	Increase protein expression of MMP inhibitor TIMP-2 and decreased ADAMTS-4
	Clinical microCT (μCT)	Decrease total microCT OA score, location and size of osteophyte, and subchondral bone sclerosis	No significant bony changes including osteophyte formation
	Quantitative microCT (μCT)	Decrease in osteophyte volumes, subchondral trabecular bone vBMD of medial tibiae and femurs	Decrease in trabecular thickness of the medial femoral condyle
	OARSI histology score	Decrease total OA score, specifically in the medial tibial compartment; contributed by articular cartilage structure, proteoglycan content and chondrocyte cellularity	Decrease total OA score, specifically in the lateral tibial compartment; contributed by articular cartilage structure, proteoglycan content and chondrocyte cellularity
	Immunohistochemistry, cartilage	Decrease protein expression of NF-κB p65 & MCP-1 inflammatory mediators in the medial tibial plateau cartilage	Increased TIMP-2 and decreased ADAMTS-4 protein expression in the cartilage of the lateral tibial plateau
	Whole joint testing	No significant changes in cranial/anterior drawer and pull to failure	No significant difference in cranial/anterior drawer. Decrease of pull to failure elastic modulus
	Cartilage indentation	Decrease in equilibrium elastic modulus in the medial femur and tibia	Decrease of instantaneous and equilibrium elastic modulus of the lateral tibial plateau
	AAS	Decreased concentrations of magnesium and phosphorous in the articular medial cartilage	Decrease of zinc in the patella and lateral articular cartilage; however, observed an increase of zinc in the patellar tendon and lateral femoral condyles

IFP/SC, infrapatellar fat pad/synovium complex; OA, osteoarthritis; FCT, fibrous connective tissue; MMP-2, matrix metallopeptidase-2; TIMP-2, tissue inhibitor of metalloproteinase-2; NF-κB, nuclear factor kappa B; MCP-1, monocyte chemoattractant protein-1; ADAMTS-4, a disintegrin and metalloproteinase with thrombospondin motifs-4; microCT, microcomputed tomography; vBMD, volumetric bone mineral density; OARSI, Osteoarthritis Research Society International; AAS, atomic absorption spectroscopy.

was tested via three techniques to identify variations in movement/mobility given the one-sided resection of the IFP/SC. To the authors' knowledge, current literature in rodent models outside of the authors' laboratory have not evaluated mobility/movement with the removal of the IFP/SC. As expected given our study in a male cohort of guinea pigs (21), treadmill and weight bearing analyses demonstrated no unilateral differences between hindlimbs in female animals. The longitudinal differences across time that were seen in gait and voluntary weight-bearing movement for both sexes were anticipated due to long-bone growth during 3 to 7 months of age (21,22,43,45).

Interestingly, overhead monitoring revealed that unilateral removal of the IFP/SC (with contralateral sham

surgery) did not hinder, and may have improved, overall voluntary movement/mobility of female guinea pigs. When control animals at 7 months of age were compared to 7-month-old females that underwent IFP/SC removal, there was a significant increase in speed, total time mobile, and total distance traveled noted; a decrease in time spent in their red hut was also observed. Increases in these parameters could indicate that guinea pigs with IFP/SC removal may have had less pain and/or physical restrictions associated with their knee joints (21). Indeed, in scenarios where conservative management of Hoffa's disease is ineffective, arthroscopic removal of the IFP/SC is pursued next (6-8). Indeed, reduction in pain is often reported following resection (46). It would be curious to determine if the pathphysiology associated with OA in this species has mechanisms in common with Hoffa's disease. Further, it would be worthwhile to pursue whether these differences may also be attributed to non-structural mechanisms and/or behavior contributions peripherally associated with OA.

It should be emphasized that the main goal of this study was to identify mechanistic contributions of the IFP to OA in an animal model and not necessarily imply its therapeutic use in humans. As it relates to humans and clinical outcomes, resection of the IFP during total knee arthroplasty (TKA) routinely occurs but is controversial. The systematic review from Yao *et al.* (47) evaluated the impact of IFP resection versus preservation on postoperative flexion, pain, Insall-Salvati ratio (ISR, ration of patellar tendon length to the patellar height), Knee Society Score (KSS, which evaluates pain based on stability and range of motion), patellar tendon length, and satisfaction in primary TKA. Of the 11,996 included cases, results provided no differences following IFP resection based on ISR, KSS, or patient satisfaction and mixed evidence for patellar tendon length, pain and knee flexion following IFP resection. Interestingly, studies of shorter follow-up intervals suggested improved pain following resection, while reports of longer follow up times indicated that resection resulted in increased pain (47). Based on the current literature, it is thus difficult to conclude whether IFP resection versus retention is preferred in cases of TKA (47). Based on the results herein, future clinical work may benefit from focusing on gender and patient mobility after resection to best indicate which technique would provide guidelines for optimal surgical outcomes in patients.

Characterization of IFP/SC versus FCT

In human clinical studies, the IFP has been studied to understand the pathophysiology of arthrofibrosis and the necessity for TKA (48-50). Macroscopically, IFP tissue in the absence of disease presents as homogenous, fatty tissue whereas IFP tissue taken at the time of TKA presents as dense, pigmented tissue (49,51,52). Histologically, tissue remodeling, inflammation (7), increased collagen deposition and increased fibroblast staining has been observed in the location where the IFP was removed at the time of TKA (49,51,52). As previously cited, Drs. Hoffa and Becker were the first to describe the replacement process as hyperplasia resulting in fibrous tissue without any intervening fat after TKA (52).

Morphologic tissue and cellular changes following removal of the IFP/SC in females of this animal model were similar to those seen in people with TKA as well as the male cohort (21). Specifically, removal of the IFP/SC resulted in FCT in this anterior location. The histomorphology of these tissues via H&E stained knee joints was further supported by transcript analysis, demonstrating decreased expression of key adipose-related molecules adiponectin, leptin, and fatty acid synthase. These same molecules were similarly decreased in the male cohort of guinea pigs. Interestingly, females in this study also showed a decrease in *CIDEC* in FCT when compared to native IFP/SC; this was not the case in males (21). *CIDEC*, or *FSP27*, mediates lipid droplet growth by promoting directional lipid transfer from smaller to larger lipid droplets (53). It has been closely linked to the development of metabolic disorders, including obesity, diabetes, and liver steatosis (54,55). *CIDEC* is most highly expressed in white and brown adipose tissues; in the context of the IFP/SC, however, there is no previous research to elucidate the role of *CIDEC*. It is reasonable to assume the decreased *CIDEC* expression with removal of the IFP/SC may be due to the lack of adipose tissue and/or droplets in the FCT. Still, the function of this mediator in the context of OA and IFP/SC removal warrants further consideration, particularly in regards to sex differences.

A focus of this study was to scrutinize the inflammatory and degradative mediator changes between the FCT and native IFP/SC. Notably, insight into how this adipose depot could contribute to OA pathogenesis in the context of obesity, meta-inflammation, and/or metabolic disease syndrome may be gleaned from the absence of signalling pathways classically associated with each of these conditions. For example, previous studies have established that elevated pro-inflammatory cytokines are among the critical mediators in OA pathogenesis (56-58); leptin, in particular, exerts a proinflammatory role (59,60). For this

female guinea pig study, leptin expression was decreased in the FCT relative to the IFP/SC; this was also true for male guinea pigs (21). Indeed, leptin levels were higher in synovial fluid and serum of OA patients compared with controls (61) and have shown a positive correlation with severity of OA (62). An *in vitro* study demonstrated that leptin increased MMP production in human OA cartilage and correlated with MMP-1 and MMP-3 in OA synovial fluid (63). Furthermore, Bao *et al.* (64), provided evidence that leptin increases the gene expression of *ADAMTS-4* and *-5* (64) as well as production of nitric oxide (NO), prostaglandin E2 (PGE2), interleukin (IL)-6 and IL-8 (64). It is thus plausible that the absence of leptin in the FCT group contributed to the improvement in joint pathology noted in this study.

MAPK pathways, in particular, play important roles in the metabolic and biomechanical pathways associated with the pathogenesis of OA (65,66). Specifically, MAPK inhibitors have been extensively studied as potential therapeutic avenue for OA treatment. In a rabbit model, enzyme papain was intra-articular injected to induce early-stage OA; investigators demonstrated that MAPK inhibitors reduced the severity of OA through significantly lower histologic OA scores and increased proteoglycan levels, as well as decreased MMP3 protein expression in cartilage (67). Interestingly, removal of IFP/SC exhibited similar findings to this study, whereby signal transcription factors, including *MAPK* gene expression, were lower in the FCT relative to native IFP/SC. In addition, we also observed a decrease in oxidative stress (*KEAP1*), antioxidant mediators (*GPx4*, *NOS3*, *Catalase*), and the complement system (*C3*), which can be regulated by converging MAPK regulated pathways (68-70).

In contrast to the male cohort, our present study demonstrated increased TIMP-2 and decreased ADAMTS-4 protein expression in FCT tissue relative to IFP/SC; these findings were also observed in the cartilage of the lateral tibial plateau. The change in expression of TIMP-2 and ADAMTS-4 in the FCT may be relevant for both cartilage degeneration and bone remodeling in female guinea pigs. OA is characterized by subchondral bone remodeling and osteophyte development as cartilage is damaged by abrasion and inflammation (32,71). Inflammatory mediators and cytokines, such as those identified above, are factors that accelerate degenerative joint disease by inducing the expression of other cartilage extracellular matrix (ECM)-degrading factors, including but not limited to iNOS, MMPs and ADAMTS-4 (63,70,72). Numerous studies have been conducted to examine the ADAMTS family. ADAMTS-4 expression is induced by proinflammatory cytokines and active forms of ADAMTS-4 were shown to be increased in synovial fluid samples of patient with OA (73,74); the related aggrecanase ADAMTS-5 has also been found to be expressed in human chondrocytes and synovial fibroblasts. Further, mice with injury induced destabilization of medial meniscus (DMM) with double-knockout of ADAMTS-4 and ADAMTS-5 had mild OA when compared to wild type mice that had developed moderate OA 8 weeks after surgery. Their findings suggest that deletion of ADAMTS-4/5 provided significant protection against proteoglycan degradation and decreased the severity of injury induced OA (73). Hashimoto *et al.* examined the inhibitory activity of TIMP-1, -2, -3 and -4 against human ADAMTS-4 in *ex vivo* OA cartilage. Collectively, their data suggest that up-regulation of TIMPs may be beneficial to halting joint degeneration (74). These existing manuscripts support the protein changes seen in our IFP/SC removal study in the female cohort. Of note, we did not observe a strong correlation to degradative mediated changes in the FCT and the native IFP in the male cohort; however, these findings justify additional studies to investigate ADAMTS and TIMP as it relates to sex differences in the IFP/SC model.

In regards to mechanical testing, our work suggested that the bone-tendon interface should be considered in the context of removal of the IFP/SC in this sex. We found that female guinea pigs demonstrated a decrease in the elastic modulus of the pull to failure test, which was a measure of both the patellar tendon and the associated FCT or IFP/SC. In an attempt to understand the relationship between tendon stiffness and failure, previous researchers conducted a meta-analysis of pooled mechanical data from representative sample of tendons from different species (75). Fifty studies were analyzed, which included healthy tendons, injured and healing tendons, genetically modified tendons, and allograft preparations; species, mechanical environment, and age were also considered. Tendons from rodents (rats and mice) and rabbits were shown to have lower elastic modulus and exhibit higher strain (noted by the higher ratio of ultimate stress to elastic modulus) (76). Further, the results confirmed that, within species, elastic modulus and ultimate stress are highly correlated, suggesting that tendon failure is highly strain dependent. Specifically, the mechanical behavior of normal/healthy and healing tendons (from transection or collagenase injection injury rodent models, respectively) confirmed that elastic modulus and ultimate stress have a strong linear correlation. Cumulatively, these

studies suggest that the lower elastic modulus of the pull to failure test in this female cohort may be attributed to the fact that the FCT was still in a state of healing and/or remodeling. Transcript and protein analyses conducted provided evidence that the FCT exhibited changes in degradative mediators, specifically MMP2. These findings would warrant further investigation into glycosaminoglycan (GAG) content within the IFP/SC and FCT tissues, which might further explain the structural integrity of these tissue types.

In an attempt to further understand the biomechanical changes seen in the FCT versus IFP/SC, we employed AAS to characterize the trace element profile in IFP/SC *vs.* FCT as well as patellae and patellar tendons. Remarkably, of the five trace elements (Ca, Mg, Zn, Fe and P) assayed, differences were only associated with Zn in the female cohort. This may be due to the role and/or function that Zn plays in the homeostasis and cellular metabolic pathways of different tissue types (76,77). In particular, it was noted that Zn increased in patellar tendons associated with knees containing the FCT. As insinuated above, these findings may be associated with tissue remodeling. Future Zn specific experimentations will need to be pursued to understand the role of this trace element in individual tissues.

Characterization of joint pathology

This work demonstrated that resection of the IFP/SC before OA development in a female cohort of a guinea pig strain that develops primary OA had short-term benefits. Notably, histopathology for OA confirmed that the knee containing the native IFP/SC was more severe relative to the knee with the replacement FCT. This finding was comparable to the male guinea pig cohort; interestingly, however, IFP/SC removal in female Dunkin Hartley guinea pigs benefited their lateral tibial compartment, whereas the male cohort OA score was attributed to improvements in their medial tibial compartment. Future studies in this OA model will focus on the influence of sex hormones on OA progression. Indeed, it has been hypothesized that sex hormones play a critical role in the progression of OA. Ma *et al.* (78) investigated the role of sex hormones in cartilage degradation in a murine model accelerated DMM. They found that sex hormones play a critical role in the progression of OA in the DMM surgical model, with males having more severe OA than females (78).

In regards to microCT findings in this female cohort, the only statistical difference identified was that the TbTh of the medial femoral condyle was significantly decreased following removal of the IFP/SC. Previous research conducted in female Dunkin Hartley guinea pigs revealed that 5-month-old animals had significantly less TbTh in their combined medial & lateral femoral condyles when compared to 1-month-old (79). The relevance of changes in TbTh of the femoral condyles outside of the context of aging is unclear; however, the presence of significant changes in more than one study indicates a potential value to considering trabecular bone changes in each individual femoral condyle.

Previous studies have reported the biomechanical/material properties of healthy human knee joint articular cartilage (80) and compared these parameters from healthy/non-OA joints OA; these manuscripts have consistently reported a decline in instantaneous and equilibrium moduli associated with the presence of OA disease (80-86). In a clinical study, these investigators provided evidence that correlations were found between site-matched cartilage and subchondral bone material properties changes during progression of aging and OA. Defining sex differences, however, was not a focus of their findings. The study presented herein demonstrated that the cartilage of the lateral tibial plateau in the knee containing the FCT had decreased indentation mechanical properties when compared to IFP/SC; this corresponded to improved OARSI histopathology scores. We previously interpreted these lower values to be more appropriate for healthy cartilage based on existing studies (21).

AAS was utilized to characterize the trace element profile in tibial cartilage as well as cortical and subchondral trabecular bone of both femoral condyles. As for AAS results described above, Zn was the only trace element with statistical differences noted in these key tissues. Here, we demonstrated that there is a decrease in Zn concentration in the lateral tibial cartilage of the knee with the FCT when compared to knee containing the native IPF/SC; these findings were associated, but not statistically correlated, with improved OA scores. In contrast, it was noted that Zn increased in the cortical and subchondral trabecular bone of the lateral femoral condyle of knees with the FCT. Previous studies have defined the hallmark of OA as the accelerated catabolism elicited by increased expression of MMPs and ADAMTSs (86). These matrix-degrading enzymes require Zn2+ for their maturation and catalytic activity, perhaps suggesting an association of intracellular Zn2+ homeostasis and OA pathogenesis (77,87). Kim *et al.* investigated the

role of Zn homeostasis as it relates to transporters and Zn-dependent transcription in OA pathogenesis (88). Collectively, they demonstrated that the zinc-ZIP8-metal transporter factor-1 (MTF1) axis in chondrocytes promotes a catabolic cascade via MMP3, MMP13, and ADAMTS5 that may incite OA. Further, their findings support that local reduction of Zn, restriction of ZIP8 function or Zn influx, and/or hindering MTF1 activity in joints could hold promise for treating OA (88,89). Our present findings lend additional support to their assertions.

There are confines to this work worthy of discussion. First, resection of the IFP/SC prior to OA provides limitations for clinical use in patients with OA. Therefore, additional time points are needed to examine the long-term benefits of IFP/SC removal during OA progression, and following end-stage disease. Second, biochemical analysis such as GAG content in conjugation with biomechanical compression analyses could provide a more comprehensive explanation to differences observed by defining the structural composition of the knee joint tissues. As previously acknowledged in our male cohort (21), the opposite knee served as a control to allow confirmation of within animal differences. Future studies will examine bilateral IFP/SC removal to reduce concerns related to compensatory limb effects. While the results from these studies are promising and show a delay in OA onset in both males and females, a longer-term study is currently underway to evaluate the potential influence of IFP/SC removal in late-stage OA.

Conclusions

Our data suggest that the IFP/SC contributes to knee OA development in female Hartley guinea pigs and that amputation of the IFP/SC prior to disease development had short-term benefits. Specifically, the formation of the FCT in place of the native tissue resulted in decreased cartilage-related OA changes, as demonstrated by reduced OARSI histology scores, as well as changes in transcript, protein, and cartilage indentation analyses. In conjuction with our report in male Hartley guinea pigs, our data provides evidence that sex needs to be considered when investigating potential responses and associated mechanisms seen with this intervention. Specifically, our results demonstrate that there are sex differences associated with early removal of IFP/SC and subsequent reduced OA development. Continued work will address findings at later stage time points in both sexes.

Acknowledgments

We would like to thank Crystal Richt and the staff at the University of Arizona Genetics Core and Kevin Daniels at Colorado State University Veterinary Diagnostic Laboratories for his assistance in generating experimental data. Additionally, we would like to thank the Department of Laboratory Animal Resources at Colorado State University for their compassion and commitment to these animals.

Funding: This work was supported by National Institute of Health (NIH) R21 AR073972 to support the acquisition, analysis, and interpretation of data. Additional funding for atomic absorption spectroscopy (AAS) was kindly supplied by the Clinical Pathology Research and Development fund at Colorado State University.

Footnote

Reporting Checklist: The authors have completed the ARRIVE reporting checklist. Available at https://atm.amegroups.com/article/view/10.21037/atm-23-1886/rc

Data Sharing Statement: Available at https://atm.amegroups.com/article/view/10.21037/atm-23-1886/dss

Peer Review File: Available at https://atm.amegroups.com/article/view/10.21037/atm-23-1886/prf

Conflicts of Interest: All authors have completed the ICMJE uniform disclosure form (available at https://atm.amegroups.com/article/view/10.21037/atm-23-1886/coif). The authors have no conflicts of interest to declare.

Ethical Statement: The authors are accountable for all aspects of the work in ensuring that questions related to the accuracy or integrity of any part of the work are appropriately investigated and resolved. Experiments were performed under a project license (#15-5854A; October 30, 2021) granted by Colorado State University's Institutional Animal Care and Use Committee, in compliance with the NIH Guide for the Care and Use of Laboratory Animals.

References

1. Chen D, Shen J, Zhao W, et al. Osteoarthritis: toward a comprehensive understanding of pathological mechanism. Bone Res 2017;5:16044.
2. Assogba TF, Niama-Natta DD, Kpadonou TG, et al. Disability and functioning in primary and secondary hip osteoarthritis in Benin. Afr J Disabil 2020;9:675.
3. Yao Q, Wu X, Tao C, et al. Osteoarthritis: pathogenic signaling pathways and therapeutic targets. Signal Transduct Target Ther 2023;8:56.
4. Hunter DJ, Bierma-Zeinstra S. Osteoarthritis. Lancet 2019;393:1745-59.
5. Ioan-Facsinay A, Kloppenburg M. An emerging player in knee osteoarthritis: the infrapatellar fat pad. Arthritis Res Ther 2013;15:225.
6. Saddik D, McNally EG, Richardson M. MRI of Hoffa's fat pad. Skeletal Radiol 2004;33:433-44.
7. Stocco E, Barbon S, Piccione M, et al. Infrapatellar Fat Pad Stem Cells Responsiveness to Microenvironment in Osteoarthritis: From Morphology to Function. Front Cell Dev Biol 2019;7:323.
8. Mace J, Bhatti W, Anand S. Infrapatellar fat pad syndrome: a review of anatomy, function, treatment and dynamics. Acta Orthop Belg 2016;82:94-101.
9. Michalak S, Łapaj Ł, Witkowska-Łuczak A, et al. Resection of Infrapatellar Fat Pad during Total Knee Arthroplasty Has No Impact on Postoperative Function, Pain and Sonographic Appearance of Patellar Tendon. J Clin Med 2022;11:7339.
10. Fontanella CG, Belluzzi E, Pozzuoli A, et al. Exploring Anatomo-Morphometric Characteristics of Infrapatellar, Suprapatellar Fat Pad, and Knee Ligaments in Osteoarthritis Compared to Post-Traumatic Lesions. Biomedicines 2022;10:1369.
11. Fontanella CG, Belluzzi E, Pozzuoli A, et al. Mechanical behavior of infrapatellar fat pad of patients affected by osteoarthritis. J Biomech 2022;131:110931.
12. Emmi A, Stocco E, Boscolo-Berto R, et al. Infrapatellar Fat Pad-Synovial Membrane Anatomo-Fuctional Unit: Microscopic Basis for Piezo1/2 Mechanosensors Involvement in Osteoarthritis Pain. Front Cell Dev Biol 2022;10:886604.
13. Stocco E, Belluzzi E, Contran M, et al. Age-Dependent Remodeling in Infrapatellar Fat Pad Adipocytes and Extracellular Matrix: A Comparative Study. Front Med (Lausanne) 2021;8:661403.
14. Klein-Wieringa IR, Kloppenburg M, Bastiaansen-Jenniskens YM, et al. The infrapatellar fat pad of patients with osteoarthritis has an inflammatory phenotype. Ann Rheum Dis 2011;70:851-7.
15. de Jong AJ, Klein-Wieringa IR, Kwekkeboom JC, et al. Inflammatory features of infrapatellar fat pad in rheumatoid arthritis versus osteoarthritis reveal mostly qualitative differences. Ann Rheum Dis 2018;77:1088-90.
16. Radakovich LB, Marolf AJ, Culver LA, et al. Calorie restriction with regular chow, but not a high-fat diet, delays onset of spontaneous osteoarthritis in the Hartley guinea pig model. Arthritis Res Ther 2019;21:145.
17. Santangelo KS, Radakovich LB, Fouts J, et al. Pathophysiology of obesity on knee joint homeostasis: contributions of the infrapatellar fat pad. Horm Mol Biol Clin Investig 2016;26:97-108.
18. Mustonen AM, Nieminen P. Fatty Acids and Oxylipins in Osteoarthritis and Rheumatoid Arthritis-a Complex Field with Significant Potential for Future Treatments. Curr Rheumatol Rep 2021;23:41.
19. Eymard F, Pigenet A, Citadelle D, et al. Induction of an inflammatory and prodegradative phenotype in autologous fibroblast-like synoviocytes by the infrapatellar fat pad from patients with knee osteoarthritis. Arthritis Rheumatol 2014;66:2165-74.
20. Kraus VB, Huebner JL, DeGroot J, et al. The OARSI histopathology initiative - recommendations for histological assessments of osteoarthritis in the guinea pig. Osteoarthritis Cartilage 2010;18 Suppl 3:S35-52.
21. Afzali MF, Radakovich LB, Sykes MM, et al. Early removal of the infrapatellar fat pad/synovium complex beneficially alters the pathogenesis of moderate stage idiopathic knee osteoarthritis in male Dunkin Hartley guinea pigs. Arthritis Res Ther 2022;24:282.
22. Boyan BD, Tosi LL, Coutts RD, et al. Addressing the gaps: sex differences in osteoarthritis of the knee. Biol Sex Differ 2013;4:4.
23. Srikanth VK, Fryer JL, Zhai G, et al. A meta-analysis of sex differences prevalence, incidence and severity of osteoarthritis. Osteoarthritis Cartilage 2005;13:769-81.
24. O'Connor MI. Sex differences in osteoarthritis of the hip and knee. J Am Acad Orthop Surg 2007;15 Suppl 1:S22-5.
25. Sokoloff L. Natural history of degenerative joint disease in small laboratory animals. I. Pathological anatomy of

degenerative joint disease in mice. AMA Arch Pathol 1956;62:118-28.
26. Davis MA. Epidemiology of osteoarthritis. Clin Geriatr Med 1988;4:241-55.
27. Vincent TL. Of mice and men: converging on a common molecular understanding of osteoarthritis. Lancet Rheumatol 2020;2:e633-45.
28. Li H, George DM, Jaarsma RL, et al. Metabolic syndrome and components exacerbate osteoarthritis symptoms of pain, depression and reduced knee function. Ann Transl Med 2016;4:133.
29. Pan F, Han W, Wang X, et al. A longitudinal study of the association between infrapatellar fat pad maximal area and changes in knee symptoms and structure in older adults. Ann Rheum Dis 2015;74:1818-24.
30. Helbling JE, Spittler AP, Sadar MJ, et al. Optimization of overhead enclosure monitoring in juvenile male Dunkin Hartley guinea pigs (Cavia porcellus). Lab Anim 2023;57:552-64.
31. Burton LH, Afzali MF, Radakovich LB, et al. Systemic administration of a pharmacologic iron chelator reduces cartilage lesion development in the Dunkin-Hartley model of primary osteoarthritis. Free Radic Biol Med 2022;179:47-58.
32. Radakovich LB, Marolf AJ, Shannon JP, et al. Development of a microcomputed tomography scoring system to characterize disease progression in the Hartley guinea pig model of spontaneous osteoarthritis. Connect Tissue Res 2018;59:523-33.
33. Batiste DL, Kirkley A, Laverty S, et al. Ex vivo characterization of articular cartilage and bone lesions in a rabbit ACL transection model of osteoarthritis using MRI and micro-CT. Osteoarthritis Cartilage 2004;12:986-96.
34. Batiste DL, Kirkley A, Laverty S, et al. High-resolution MRI and micro-CT in an ex vivo rabbit anterior cruciate ligament transection model of osteoarthritis. Osteoarthritis Cartilage 2004;12:614-26.
35. Fischenich KM, Button KD, DeCamp C, et al. Comparison of two models of post-traumatic osteoarthritis; temporal degradation of articular cartilage and menisci. J Orthop Res 2017;35:486-95.
36. Pauly HM, Larson BE, Coatney GA, et al. Assessment of cortical and trabecular bone changes in two models of post-traumatic osteoarthritis. J Orthop Res 2015;33:1835-45.
37. Idleburg C, DeLassus EN, Novack DV. Immunohistochemistry of skeletal tissues. Methods Mol Biol 2015;1226:87-95.
38. Helrich K, editor. Association of Official Analytical Chemists. Official Methods of Analysis of AOAC International. 15th ed. Gaithersburg, MD, USA; AOAC International; 1990. Official method 968.08D.
39. Lim NH, Kashiwagi M, Visse R, et al. Reactive-site mutants of N-TIMP-3 that selectively inhibit ADAMTS-4 and ADAMTS-5: biological and structural implications. Biochem J 2010;431:113-22.
40. Verma P, Dalal K. ADAMTS-4 and ADAMTS-5: key enzymes in osteoarthritis. J Cell Biochem 2011;112:3507-14.
41. Valdrighi N, Blom AB, van Beuningen HM, et al. Early pain in females is linked to late pathological features in murine experimental osteoarthritis. PeerJ 2023;11:e15482.
42. Wu J, Pan Y, Yu Y, et al. Axial Compressive Loading Attenuates Early Osteoarthritis by Reducing Subchondral Bone Remodeling. Am J Sports Med 2023;51:1752-64.
43. Afzali MF, Pannone SC, Martinez RB, et al. Intravenous injection of adipose-derived mesenchymal stromal cells benefits gait and inflammation in a spontaneous osteoarthritis model. J Orthop Res 2023;41:902-12.
44. Pezzanite LM, Timkovich AE, Sikes KJ, et al. Erythrocyte removal from bone marrow aspirate concentrate improves efficacy as intra-articular cellular therapy in a rodent osteoarthritis model. Ann Transl Med 2023;11:311.
45. Musci RV, Andrie KM, Walsh MA, et al. Phytochemical compound PB125 attenuates skeletal muscle mitochondrial dysfunction and impaired proteostasis in a model of musculoskeletal decline. J Physiol 2023;601:2189-216.
46. Doner GP, Noyes FR. Arthroscopic resection of fat pad lesions and infrapatellar contractures. Arthrosc Tech 2014;3:e413-6.
47. Yao B, Samuel LT, Acuña AJ, et al. Infrapatellar Fat Pad Resection or Preservation during Total Knee Arthroplasty: A Systematic Review. J Knee Surg 2021;34:415-21.
48. Unterhauser FN, Bosch U, Zeichen J, et al. Alpha-smooth muscle actin containing contractile fibroblastic cells in human knee arthrofibrosis tissue. Winner of the AGA-DonJoy Award 2003. Arch Orthop Trauma Surg 2004;124:585-91.
49. Abdul N, Dixon D, Walker A, et al. Fibrosis is a common outcome following total knee arthroplasty. Sci Rep 2015;5:16469.
50. Bayram B, Limberg AK, Salib CG, et al. Molecular pathology of human knee arthrofibrosis defined by RNA sequencing. Genomics 2020;112:2703-12.
51. Kumar D, Alvand A, Beacon JP. Impingement of infrapatellar fat pad (Hoffa's disease): results of high-

portal arthroscopic resection. Arthroscopy 2007;23:1180-1186.e1.
52. Hoffa A. The Influence of the Adipose Tissue with Regard to the Pathology of the Knee Joint. JAMA 1904;43:795-6.
53. Gong J, Sun Z, Wu L, et al. Fsp27 promotes lipid droplet growth by lipid exchange and transfer at lipid droplet contact sites. J Cell Biol 2011;195:953-63.
54. Gong J, Sun Z, Li P. CIDE proteins and metabolic disorders. Curr Opin Lipidol 2009;20:121-6.
55. Puri V, Czech MP. Lipid droplets: FSP27 knockout enhances their sizzle. J Clin Invest 2008;118:2693-6.
56. Clockaerts S, Bastiaansen-Jenniskens YM, Runhaar J, et al. The infrapatellar fat pad should be considered as an active osteoarthritic joint tissue: a narrative review. Osteoarthritis Cartilage 2010;18:876-82.
57. Balistreri CR, Caruso C, Candore G. The role of adipose tissue and adipokines in obesity-related inflammatory diseases. Mediators Inflamm 2010;2010:802078.
58. Bravo B, Guisasola MC, Vaquero J, et al. Gene expression, protein profiling, and chemotactic activity of infrapatellar fat pad mesenchymal stem cells in pathologies of the knee joint. J Cell Physiol 2019;234:18917-27.
59. Collins KH, Lenz KL, Pollitt EN, et al. Adipose tissue is a critical regulator of osteoarthritis. Proc Natl Acad Sci U S A 2021;118:e2021096118.
60. Moverley R, Williams D, Bardakos N, et al. Removal of the infrapatella fat pad during total knee arthroplasty: does it affect patient outcomes? Int Orthop 2014;38:2483-7.
61. Sachdeva M, Aggarwal A, Sharma R, et al. Chronic inflammation during osteoarthritis is associated with an increased expression of CD161 during advanced stage. Scand J Immunol 2019;90:e12770.
62. Abdelnaby R, Sonbol YT, Dardeer KT, et al. Could Osteopontin be a useful biomarker in the diagnosis and severity assessment of osteoarthritis? A systematic review and meta-analysis of recent evidence. Clin Immunol 2023;246:109187.
63. Koskinen A, Vuolteenaho K, Nieminen R, et al. Leptin enhances MMP-1, MMP-3 and MMP-13 production in human osteoarthritic cartilage and correlates with MMP-1 and MMP-3 in synovial fluid from OA patients. Clin Exp Rheumatol 2011;29:57-64.
64. Bao JP, Chen WP, Feng J, et al. Leptin plays a catabolic role on articular cartilage. Mol Biol Rep 2010;37:3265-72.
65. Du XF, Huang K, Chen XY, et al. Gremlin-1 promotes IL-1β-stimulated chondrocyte inflammation and extracellular matrix degradation via activation of the MAPK signaling pathway. J Biochem Mol Toxicol 2023;37:e23404.
66. Wan J, Li M, Yuan X, et al. Rutaecarpine ameliorates osteoarthritis by inhibiting PI3K/AKT/NF-κB and MAPK signalling transduction through integrin αVβ3. Int J Mol Med 2023;52:97.
67. Lan CN, Cai WJ, Shi J, et al. MAPK inhibitors protect against early-stage osteoarthritis by activating autophagy. Mol Med Rep 2021;24:829.
68. Xu B, Lang LM, Lian S, et al. Oxidation Stress-Mediated MAPK Signaling Pathway Activation Induces Neuronal Loss in the CA1 and CA3 Regions of the Hippocampus of Mice Following Chronic Cold Exposure. Brain Sci 2019;9:273.
69. Tabarsa M, Dabaghian EH, You S, et al. Inducing inflammatory response in RAW264.7 and NK-92 cells by an arabinogalactan isolated from Ferula gummosa via NF-κB and MAPK signaling pathways. Carbohydr Polym 2020;241:116358.
70. Kang EH, Lee YJ, Kim TK, et al. Adiponectin is a potential catabolic mediator in osteoarthritis cartilage. Arthritis Res Ther 2010;12:R231.
71. Li G, Yin J, Gao J, et al. Subchondral bone in osteoarthritis: insight into risk factors and microstructural changes. Arthritis Res Ther 2013;15:223.
72. Wang T, He C. Pro-inflammatory cytokines: The link between obesity and osteoarthritis. Cytokine Growth Factor Rev 2018;44:38-50.
73. Tortorella MD, Arner EC, Hills R, et al. Alpha2-macroglobulin is a novel substrate for ADAMTS-4 and ADAMTS-5 and represents an endogenous inhibitor of these enzymes. J Biol Chem 2004;279:17554-61.
74. Hashimoto G, Aoki T, Nakamura H, et al. Inhibition of ADAMTS4 (aggrecanase-1) by tissue inhibitors of metalloproteinases (TIMP-1, 2, 3 and 4). FEBS Lett 2001;494:192-5.
75. LaCroix AS, Duenwald-Kuehl SE, Lakes RS, et al. Relationship between tendon stiffness and failure: a metaanalysis. J Appl Physiol (1985) 2013;115:43-51.
76. Sharma P, Maffulli N. Biology of tendon injury: healing, modeling and remodeling. J Musculoskelet Neuronal Interact 2006;6:181-90.
77. Andreini C, Banci L, Bertini I, et al. Counting the zinc-proteins encoded in the human genome. J Proteome Res 2006;5:196-201.
78. Ma HL, Blanchet TJ, Peluso D, et al. Osteoarthritis severity is sex dependent in a surgical mouse model. Osteoarthritis Cartilage 2007;15:695-700.
79. Kim SJ, Kim JE, Choe G, et al. Self-assembled peptide-substance P hydrogels alleviate inflammation and

ameliorate the cartilage regeneration in knee osteoarthritis. Biomater Res 2023;27:40.
80. Petitjean N, Canadas P, Royer P, et al. Cartilage biomechanics: From the basic facts to the challenges of tissue engineering. J Biomed Mater Res A 2023;111:1067-89.
81. Kleemann RU, Krocker D, Cedraro A, et al. Altered cartilage mechanics and histology in knee osteoarthritis: relation to clinical assessment (ICRS Grade). Osteoarthritis Cartilage 2005;13:958-63.
82. Wilusz RE, Zauscher S, Guilak F. Micromechanical mapping of early osteoarthritic changes in the pericellular matrix of human articular cartilage. Osteoarthritis Cartilage 2013;21:1895-903.
83. Hori RY, Mockros LF. Indentation tests of human articular cartilage. J Biomech 1976;9:259-68.
84. Franz T, Hasler EM, Hagg R, et al. In situ compressive stiffness, biochemical composition, and structural integrity of articular cartilage of the human knee joint. Osteoarthritis Cartilage 2001;9:582-92.
85. Wang M, Peng Z, Price J, et al. Study of the nano-mechanical properties of human knee cartilage in different wear conditions. Wear 2013;301:188-91.
86. Zuo Q, Lu S, Du Z, et al. Characterization of nano-structural and nano-mechanical properties of osteoarthritic subchondral bone. BMC Musculoskelet Disord 2016;17:367.
87. Page-McCaw A, Ewald AJ, Werb Z. Matrix metalloproteinases and the regulation of tissue remodelling. Nat Rev Mol Cell Biol 2007;8:221-33.
88. Kim JH, Jeon J, Shin M, et al. Regulation of the catabolic cascade in osteoarthritis by the zinc-ZIP8-MTF1 axis. Cell 2014;156:730-43.
89. Fukada T, Yamasaki S, Nishida K, et al. Zinc homeostasis and signaling in health and diseases: Zinc signaling. J Biol Inorg Chem 2011;16:1123-34.

Cite this article as: Afzali MF, Sykes MM, Burton LH, Patton KM, Lee KR, Seebart C, Vigon N, Ek R, Narez GE, Marolf AJ, Sikes KJ, Haut Donahue TL, Santangelo KS. Removal of the infrapatellar fat pad and associated synovium benefits female guinea pigs in the Dunkin Hartley model of idiopathic osteoarthritis. Ann Transl Med 2024;12(3):43. doi: 10.21037/atm-23-1886

